Microb Ecol (2012) 63:74–84
DOI 10.1007/s00248-011-9935-3

ENVIRONMENTAL MICROBIOLOGY

Environmental Controls on Microbial Abundance and Activity on the Greenland Ice Sheet: A Multivariate Analysis Approach

Marek Stibal · Jon Telling · Joe Cook · Ka Man Mak · Andy Hodson · Alexandre M. Anesio

Received: 3 June 2011 / Accepted: 22 August 2011 / Published online: 7 September 2011

Abstract Microbes in supraglacial ecosystems have been proposed to be significant contributors to regional and possibly global carbon cycling, and quantifying the biogeochemical cycling of carbon in glacial ecosystems is of great significance for global carbon flow estimations. Here we present data on microbial abundance and productivity, collected along a transect across the ablation zone of the Greenland ice sheet (GrIS) in summer 2010. We analyse the relationships between the physical, chemical and biological variables using multivariate statistical analysis. Concentrations of debris-bound nutrients increased with distance from the ice sheet margin, as did both cell numbers and activity rates before reaching a peak (photosynthesis) or a plateau (respiration, abundance) between 10 and 20 km from the margin. The results of productivity measurements suggest an overall net autotrophy on the GrIS and support the proposed role of ice sheet ecosystems in carbon cycling as regional sinks of CO_2 and places of production of organic matter that can be a potential source of nutrients for downstream ecosystems. Principal component analysis based on chemical and biological data revealed three clusters of sites, corresponding to three 'glacier ecological zones', confirmed by a redundancy analysis (RDA) using physical data as predictors. RDA using data from the largest 'bare ice zone' showed that glacier surface slope, a proxy for melt water flow, accounted for most of the variation in the data. Variation in the chemical data was fully explainable by the determined physical variables. Abundance of phototrophic microbes and their proportion in the community were identified as significant controls of the carbon cycling-related microbial processes.

M. Stibal (✉) · J. Telling · K. M. Mak · A. M. Anesio
Bristol Glaciology Centre, School of Geographical Sciences,
University of Bristol,
University Road,
Bristol BS8 1SS, UK
e-mail: marek.stibal@bristol.ac.uk

J. Cook · A. Hodson
Department of Geography, University of Sheffield,
Sheffield, UK

Introduction

Significant numbers of active microbes have been found on the surface of the Greenland ice sheet (GrIS), the second largest body of ice on Earth [10, 25], and on other ice sheets and glaciers worldwide [1, 6, 9]. Supraglacial (glacier surface) ecosystems have been proposed to be potential contributors to regional and possibly global carbon cycling owing to their large area and autochthonous production of labile organic matter [1, 11]. They are also among the fastest changing on our planet [16, 35], and the rapid loss of glacier ice from the Earth's surface means that there will be a shift from glacial to proglacial environments where carbon is likely to be sequestered and cycled in a different manner to glaciers. Quantifying the biogeochemical cycling of carbon in glacial ecosystems at present is, therefore, of great significance for global carbon flow estimations and predicting future change.

First estimates of the contribution of glaciers to carbon flows have recently been published. Anesio et al. [1] scaled up the production rates determined at several small valley glaciers to all glacier surfaces outside of Antarctica and suggested that Arctic glacier surfaces are net autotrophic and sinks of ~60 Gg of atmospheric carbon per year. This would mean that the productivity of supraglacial ecosystems is comparable to other oligotrophic freshwater and soil ecosystems in boreal and temperate areas [1]. Hodson et al.

[10] measured microbial production at the margin of the GrIS and estimated an annual carbon source of ~5 Gg C per year (i.e. net heterotrophy). Stibal et al. [25] found that the amount and quality of organic carbon (OC) on the surface of the GrIS have significant spatial variability and speculated that they may be controlled by simple factors—aeolian input of microbial inoculum and nutrients, biological carbon transformation on the ice and the wash-away of supraglacial debris by meltwaters. Therefore, in order to refine the glacial productivity estimates, it is important to account for spatial variation of productivity on large ice sheets such as the GrIS and for its possible environmental controls.

In this paper, we address the spatial variation issue by measuring microbial abundance and productivity along a transect across the entire ablation zone of the GrIS (~70 km). For the in situ productivity measurements, we use the total dissolved inorganic carbon (ΔTDIC) method [9] that has recently been identified as the most appropriate for these supraglacial environments [28]. We then analyse the data using multivariate statistical analysis in order to identify significant environmental controls of microbial processes. Multivariate analysis is a powerful tool for analysing variation in large datasets with many environmental and biological variables, and its use in microbial ecology is on the rise [17]. Various methods of multivariate analysis have been used in both exploratory and explanatory microbiological studies from numerous environments, including soils [3, 18] and freshwater biofilms [14]. Constrained ordination methods (RDA, CCA) have also been used in supraglacial environments to explain the variation within microbial abundance data on several glaciers in the Arctic and Antarctic [5, 12, 15, 21]. By identifying the most significant physical variables for microbial productivity, we aim to inform biogeochemical modelling of carbon balance of the ice sheet and thus contribute to the knowledge of carbon cycling in the cryosphere and the role of microbes in this very important process.

Methods

Data Collection and Analysis

All data were collected in August 2010 along a linear transect across the ablation zone of the southwest part of the GrIS, starting at the front of Leverett Glacier and stretching up to ~70 km into the ice sheet (Fig. 1). Leverett Glacier and the transect have been described in detail in a recent paper [25]. Four randomly selected sites at each transect point were used for 24-h in situ measurements of productivity and collection of debris and water samples.

The following characteristics were determined and used as physical variables. First, distance from the front of Leverett Glacier (D_{Lev}) that occupies a valley and thus is likely to form a principal route for wind and transport of material, and second, distance from the nearest spot of deglaciated land (D_{degl}) were measured using hand-held GPS generated data. Both are considered here proxies for input of microbial propagules and rock-derived nutrients from local sources and both were included in the initial analysis in order to infer whether simple distance (D_{degl}) or the prevailing wind path (D_{Lev}) is of greater ecological significance. Third, altitude was also recorded by a hand-held GPS and is considered a proxy for average air temperature and so the duration of melting and, therefore, growing season. Fourth, slope at a given point (S) was calculated as follows:

$$S = \arctan(\Delta A/\Delta D)$$

where ΔA is the difference in altitude between points surrounding the given point and ΔD the horizontal distance between them. Additional GPS points at the front of

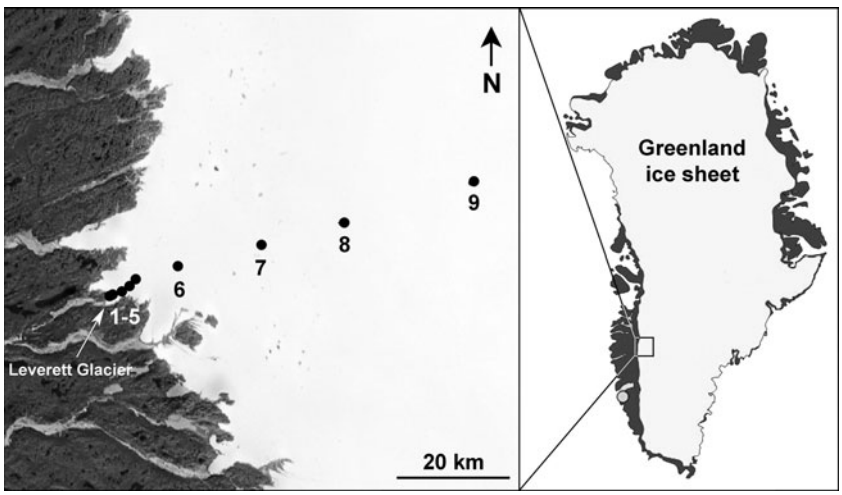

Figure 1 Transect from the front of Leverett Glacier to ~70 km into the Greenland ice sheet, with marked sampling points

Leverett Glacier and at ~100 km from the front were determined and used for the calculations. Although slope is directly dependent on distance and altitude, it may have important ecological significance due to its direct effect on water flow intensity and thus the 'wash-away' effect [25], and so was included in the analysis.

Cryoconite debris coverage of the glacier surface was determined by removing debris from the glacier surface by a flame-sterilised spatula and from cryoconite holes and slush using a 100-ml syringe, filtering through a 0.45-mm filter, oven drying at 30°C and weighing [8]. The debris coverage is the result of the physical processes of avalanching of material from adjacent slopes, wind deposition of dust, melting out of old debris and water transport of the debris down glacier [2, 10, 25], and so is likely dependent on both distance and slope. It is also a useful marker for dividing the ice sheet into 'glacier ecological zones' [10, 25]. The marginal zone along the edge of the ice sheet is directly affected by material avalanching from nearby slopes and by subglacial material, and cryoconite holes are not formed here. The bare ice zone is characterised by developed cryoconite holes and meltwater streams, while in the slush zone, the surface is covered in melting snow, and cryoconite holes and streams are not developed. Both the bare ice zone and the slush zone only receive wind-borne debris [2, 10].

The following chemical properties were determined in samples from each site: debris-bound OC, total nitrogen (TN) and exchangeable ammonia, and porewater nitrate (NO_3^-), ammonia (NH_4^+) and soluble reactive phosphorus (SRP). The total carbon (TC) and TN contents of the debris were determined using a EuroVector EA3000 Elemental Analyser (EuroVector, Milan, Italy). Inorganic carbon was measured on a Ströhlein Coulomat 702 analyser (Ströhlein Instruments, Kaarst, Germany) adapted for this purpose. Both analysers were calibrated using certified standards. Detection limits were 10 ppm for both elements, and the precision of determinations was 0.3%. The OC content was calculated as the difference between TC and inorganic carbon content. The exchangeable ammonia and porewater nutrient data are from Telling et al. (submitted for publication).

Abundance of bacteria and viruses was determined after staining with the DNA stain SYBR Gold and filtering through 0.2 and 0.02 μm filters, respectively. Ten milligrams of freshly melted cryoconite debris and 1 ml of pre-sterilised deionised water were placed in a sterile Eppendorf tube and mixed by vortexing for 30 s; 0.2 (for bacterial counts) and 0.02 (for viruses) μm filter-sterilised 37% formaldehyde (final concentration 1%) was added to the tube to fix the sample. The suspension was filtered onto a sterile Anodisc filter (Whatman, Maidstone, UK). Dried filters were placed onto 100 μl drops of 2× SYBR Gold (Invitrogen, Eugene, OR, USA) for 15 min, dried and mounted on microscopic slides with the anti-fade agent Citifluor AF2 (Citifluor, Leicester, UK). More than 300 SYBR Gold-stained cells were enumerated on each slide with an Olympus BX41 epifluorescence microscope (Olympus Optical, Tokyo, Japan) using the filter block U-N31001 (excitation 480 nm, emission 535 nm; Chroma Technology, Rockingham, VT, USA). A procedural blank with no sediment was counted in parallel and the average blank counts were then subtracted from the experimental sample counts. Photoautotrophic microbes were enumerated in non-stained samples using chlorophyll autofluorescence and the filter block U-MWU2 (excitation 330–385 nm, emission 420+; Olympus Optical, Tokyo, Japan) and classified into cyanobacteria (Oscillatoriales and Nostocales), green algae (Chlorophyceae) and desmids (Zygnematophyceae) on the basis of their morphology [12].

Net ecosystem production (NEP) and respiration (R) were measured with the ΔTDIC method, optimised specifically for this purpose [9, 28]. Cryoconite debris was collected at each site and placed into 60 ml BOD bottles with tapered glass stoppers to give an in situ debris/water ratio (approximately 1:60 [28]). Dark bottles for respiration measurements were covered with aluminium foil while the light bottles for NEP measurements were illuminated by natural light. All bottles were completely submerged in water within cryoconite holes and incubated for 24±1 h. Starting values for TDIC were established by filling three identical BOD bottles with supraglacial water and measuring immediately for TDIC with an EGM-4 infrared CO_2 metre (PP Systems, Amesbury, MT, USA). TDIC was then measured in all the bottles at the end of the incubation period. All measurements were made in situ on the ice sheet immediately after removing the bottles from the cryoconite holes. Corrections for carbonate dissolution during incubation were made following the procedure of Hodson et al. [9]. Start and end incubation concentrations of Ca^{2+} and Mg^{2+} were measured on a Dionex 4000i ion chromatography system (Dionex, Camberley, UK). The acidified samples were stored refrigerated for up to 4 months prior to analysis. The detection limits for Ca^{2+} and Mg^{2+} were 2.0 and 0.93 μM, respectively. NEP and R were then determined as ΔTDIC in light and dark bottles, respectively. Gross photosynthesis (PP) rates were calculated as NEP+R. The rates were normalised for the different dry weights of sediment in the bottles, determined by drying and weighing the sediment. The detection limits were 1.2 μg C g^{-1} day^{-1} for NEP and R and 1.7 μg C g^{-1} day^{-1} for PP. Nitrogen fixation was determined in situ using the field-adapted acetylene method of Telling et al. [29]. Nitrogen fixation data are from Telling et al. (submitted for publication).

Statistical Analysis

The glacier ecological zones (marginal, bare ice, slush) were used as dummy variables in the analysis. Distance, slope, coverage and all the chemical data were ln(x+1) transformed, as were the abundance and activity data, except for the specific PP and R rates. The phototroph proportion (percent) data were arcsin$\sqrt{x}$ transformed. All data were standardised and centred. Sample or species columns with missing data (n.d.) were removed from the analysis. Data below the detection limit (b.d.) were treated as zeros.

The data were analysed with a combination of constrained and unconstrained multivariate statistical methods in order to account for both total variation in the data and variation explainable by the environmental data. Detrended correspondence analysis (DCA) and detrended canonical correspondence analysis (DCCA) were used to determine the length of the gradient along the first ordination axis in order to select the appropriate method for unconstrained and constrained ordination of the data, respectively.

Principal component analysis (PCA) was employed to analyse the total variation in the chemistry and microbial abundance and activity data and to discern patterns within the dataset. PCA describes the axes of maximum variability in the multivariate dataset. Relationships between environmental variables and the multivariate data are quantified indirectly through regression of environmental gradients on ordination axes.

RDA can be used for ecological interpretation of data, i.e. to assess the significance of multiple environmental variables as controls for biological processes [17]. RDA is a constrained ordination technique, based on PCA, in which ordination axes are constrained to be linear combinations of environmental variables [30]. Thus, RDA allows direct assessment of the relationship between known environmental variables and variation in the multivariate data. The significance of the relationship is tested with the Monte Carlo permutation test [31]. We used the following RDA setup: focus on sample distances, 499 Monte Carlo permutations in the split-plot mode restricted for linear transect and manual forward selection. In forward selection, the construction of the regression model starts with the environmental variable that explains the most variation in the dependent variables. What remains of the variation to explain after fitting the first variable is then used to choose the second environmental variable. The process of selection goes on until no more variables significantly explain the residual variation. This allows to select the most significant variables and to avoid the problem of multicollinearity [13, 17].

All the analyses were performed in the multivariate data analysis software CANOCO 4.5. The program CANODRAW 4.0 [31] was used for graphical presentation of ordination results. The results of RDA were summarised using biplot diagrams. In the biplot diagram, the relative length and position of arrows show the extent and direction of response of the selected dependent variables to the environmental factors.

Results

Environmental Data from the GrIS Transect

Tables 1, 2 and 3 show the means and standard deviations (n=4) of the physical, chemical and microbial abundance and activity data measured along the transect and used for the multivariate statistical analysis. The physical parameters were determined, samples collected and activity measurements performed at nine transect points spanning from the front of Leverett Glacier at 399 m a.s.l. in the marginal ice zone through the bare ice zone containing cryoconite holes to the slush zone ~70 km inland at >1,400 m a.s.l. (Figure 1). The zones were clearly distinguished by the coverage of the surface debris, with a 100% (~3,800 gm^{-2}) coverage of debris in the marginal ice zone, between 0.7% and 6.4% of the area (27–240 gm^{-2}) in the bare ice zone, and with virtually no surface debris in the slush zone (Table 1).

Debris-bound organic carbon and both total nitrogen and exchangeable ammonia increased with distance and altitude, corresponding to results from previous years [25, 33].

Table 1 Physical properties of the transect points

Transect point	1	2	3	4	5	6	7	8	9
Glacier ecological zone	Marginal ice	Bare ice							Slush
D_{degl} [km]	0	0.4	2	3.6	5.4	11	27	42	65
D_{Lev} [km]	0	2	4	5.7	7.5	17	34	51	79
Altitude [m a.s.l.]	399	415	421	540	586	761	1022	1186	1446
Slope [°]	1.83	2.88	1.93	1.75	1.16	0.93	0.71	0.54	0.45
Debris coverage [g m^{-2}]	3,800	27	52	77	64	75	180	240	0

D_{Lev} distance from the terminus of Leverett Glacier, D_{degl} distance from nearest deglaciated land

Table 2 Nutrient concentrations at the transect points

Transect point	1	2	3	4	5	6	7	8	9
OC [mg g^{-1}]	0.97±0.28	2.7±1.2	3.8±0.61	5.6±1.0	15±1.1	47±1.8	62±4.3	65±3.2	n.d.
TN [mg g^{-1}]	b.d.	0.46±0.02	0.53±0.11	0.63±0.06	1.5±0.12	4.1±0.13	5.3±0.24	6.5±0.40	n.d.
NH_4-N[a] [μg g^{-1}]	b.d.	b.d.	0.33±0.65	b.d.	1.4±0.95	9.2±1.2	9.2±0.49	12±1.7	n.d.
NO_3^{-}[a] [μg l^{-1}]	n.d.	b.d.	3.9±3.1	3.6±3.5	8.0±2.5	11±4.8	11±6.0	11±0.47	12±0.9
NH_4^{+}[a] [μg l^{-1}]	n.d.	b.d.	12±3.2	0.80±1.6	2.9±4.4	b.d.	b.d.	b.d.	b.d.
SRP[a] [μg l^{-1}]	n.d.	b.d.	b.d.	b.d.	b.d.	b.d.	b.d.	b.d.	b.d.

OC debris-bound organic carbon, *TN* debris-bound total nitrogen, *NH_4-N* debris-bound exchangeable ammonia, *NO_3^-* porewater nitrate, *NH_4^+* porewater ammonia, *SRP* soluble reactive phosphorus, *b.d.* below detection, *n.d.* not determined due to insufficient amount of sample

[a] Data from Telling et al. (submitted for publication)

Both porewater NH_4^+ and NO_3^- concentrations ranged from below detection to ~12 μg N l^{-1}, and no soluble reactive phosphorus was detected in any sample (i.e. <10 μg P l^{-1}; Table 2) (Telling et al., submitted for publication).

The total microbial abundance ranged from 24 to 440 × 10^6 cells per g of debris, and the proportion of phototrophic microbes was between 1.2% and 32%. Members of two cyanobacterial groups, Oscillatoriales and Nostocales, were found, together with green coccoid algae and saccoderm desmids, typical for glacier surface habitats [21, 32, 34]. The rates of photosynthesis ranged from 1.8 to 58 μg C g^{-1} day^{-1} and the cell-specific photosynthesis was between 0.75 and 8.5 pg C $cell^{-1}$ day^{-1}. Respiration rates per unit mass of cryoconite debris were between 0.42 and 41 μg C g^{-1} day^{-1} and specific respiration rates 8.5–280 fg C $cell^{-1}$ day^{-1}. Gross photosynthesis rates were higher or not significantly lower than respiration rates at all sites, indicating net autotrophy. Figure 2 shows the abundance of phototrophs and heterotrophs and the mass- and cell-specific rates of photosynthesis and respiration plotted against the distance from the front of Leverett Glacier (D_{Lev}). Both cell numbers and activity rates increase with increasing distance up to 10–20 km from the ice sheet margin. Photosynthesis rates peak here, while the abundance of both phototrophs and heterotrophs and rates of respiration reach a plateau.

Figure 3 shows the net ecosystem production per unit area (in milligrams carbon per square metre of glacier

Table 3 Microbial abundance and activity at the transect points

Transect point	1	2	3	4	5	6	7	8	9
Microbial abundance [10^6 cells g^{-1}]									
Heterotrophs	37±14	86±31	180±39	74±47	220±79	240±180	100±26	120±58	100±14
Phototrophs	0.59±0.08	15±1.5	12±2.1	16±10	28±0.17	27±6.5	24±0.37	33±3.8	n.d.
Cyanobacteria	0.20±0.09	14±1.5	9.5±2.5	12±11	24±0.85	23±6.2	18±1.4	28±3.9	n.d.
Oscillatoriales	0.13±0.19	14±1.2	8.4±3.0	8.7±12	23±0.21	17±4.9	16±1.6	27±5.3	n.d.
Nostocales	0.06±0.09	0.20±0.28	1.2±0.47	2.9±1.1	1.5±0.64	5.8±1.3	2.0±0.14	0.98±1.4	n.d.
Chlorophyceae	0.22±0.03	0.73±0.04	1.4±0.20	1.5±0.34	2.2±0.36	2.5±0.38	3.9±1.9	3.0±0.47	n.d.
Zygnematophyceae	0.17±0.02	0.58±0.02	1.3±0.25	3.2±1.5	1.2±0.32	1.8±0.11	1.5±0.16	1.7±0.32	n.d.
% Phototrophs	1.8±0.68	16±4.9	6.6±1.2	22±11	12±4.0	15±10	19±3.7	23±8.5	n.d.
Viruses	75±7.4	190±130	47±25	13±6.2	190±53	75±27	200±47	61±6.7	n.d.
Microbial activity									
NEP [μg C g^{-1} day^{-1}]	1.9±0.88	1.9±2.7	3.2±2.0	2.8±1.1	8.5±7.9	22±4.8	6.1±2.6	2.5±2.0	b.d.
PP [μg C g^{-1} day^{-1}]	3.1±1.6	14±3.1	24±3.1	17±1.1	29±6.7	48±8.1	27±10	34±5.2	b.d.
R [μg C g^{-1} day^{-1}]	1.2±1.1	12±1.5	20±2.1	15±0	20±11	26±6.6	21±11	32±6.3	b.d.
Specific PP [pg C $cell^{-1}$ d^{-1}]	5.3±2.6	0.94±0.21	1.9±0.25	1.1±0.06	1.1±0.24	1.8±0.30	1.2±0.44	1.1±0.16	n.d.
Specific R [fg C $cell^{-1}$ day^{-1}]	35±29	130±43	110±23	200±98	92±37	140±84	170±92	220±64	n.d.
N_2 fixation[a] [ng N g^{-1} day^{-1}]	17±2.6	59±68	b.d.	16±12	b.d.	b.d.	b.d.	b.d.	n.d.

All values mean ± SD (n=4)

NEP net ecosystem production, *PP* photosynthesis, *R* respiration, *b.d.* below detection, *n.d.* not determined due to insufficient amount of sample

[a] Data from Telling et al. (submitted for publication)

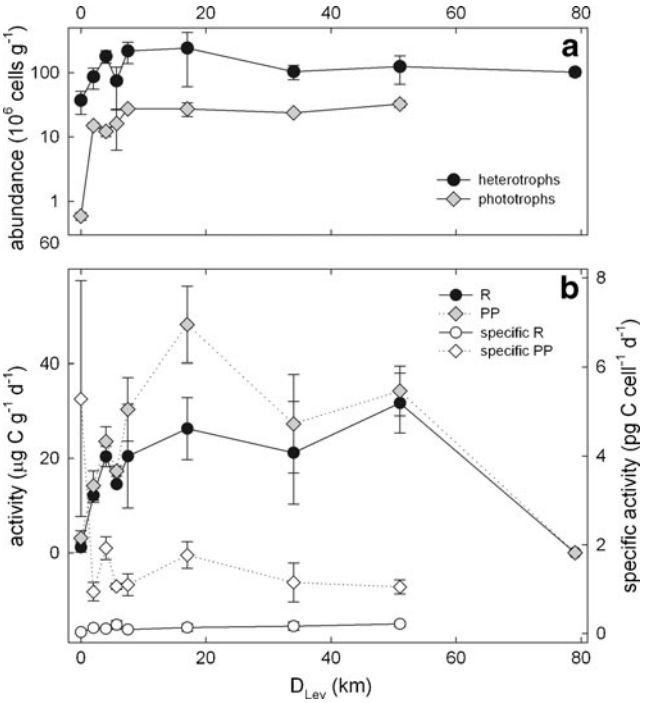

Figure 2 **a** Abundance of heterotrophic and phototrophic microbes and **b** their photosynthetic (*PP*) and respiration (*R*) activity (mean ± SD) plotted against their distance from the front of Leverett Glacier (D_{Lev}). Note the logarithmic scale in **a**

surface per day), calculated using the NEP values from Table 3 and debris coverage from Table 1 and plotted against D_{Lev}. The highest NEP per unit area (~7 mg C m^{-2} day^{-1}) was in the marginal zone, mainly due to the very high debris coverage. There was a clear trend within the data from the bare ice zone, with the NEP values steadily increasing from the margin to ~20 km inland, where a peak of ~1.7 mg C m^{-2} day^{-1} was reached, and then decreasing towards the slush zone. The calculated times of potential autochthonous OC accumulation based on the debris-bound OC concentrations from Table 2 and the NEP values from Table 3 are also shown in Fig. 3. They are between ~500 days at the margin, corresponding to ~4 melt seasons of 130 days [27], and >40,000 days at ~50 km inland, corresponding to ~1,500 melt seasons of 30 days.

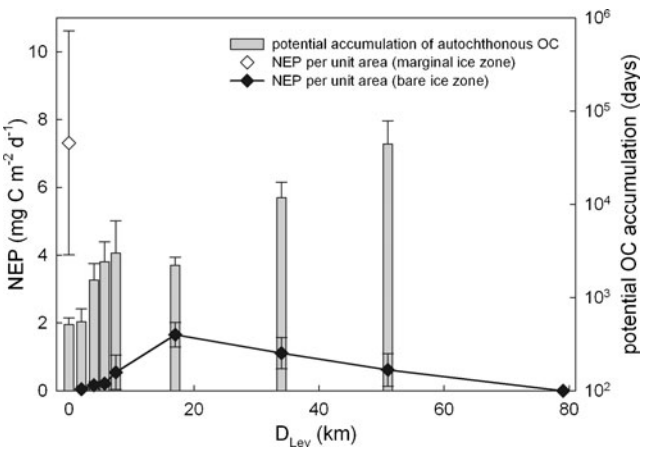

Figure 3 Net ecosystem production (*NEP*) per unit area and the potential accumulation of autochthonous organic carbon (mean ± SD) plotted against their distance from the front of Leverett Glacier (D_{Lev}). Note the logarithmic scale for the accumulation times (in days)

Multivariate Statistical Analysis

The length of the gradient along the first ordination axis of the chemical and biological data determined by DCA was 3.394 SD, and the gradient length of all the data analysed by DCCA was 2.999 SD. Linear ordination methods are recommended when the gradient length is <3 SD, and both linear and unimodal methods can be used when it is between 3 and 4 SD. Linear methods are also recommended when absolute values are analysed, as opposed to relative values [17, 31]. Therefore, the linear methods (PCA and RDA, respectively) were used for both unconstrained and constrained ordination of our data.

Figure 4 shows the results of PCA using all available chemistry (Table 2) and microbial abundance and activity (Table 3) data for each site. The first principal component explained 58% and the second principal component 11% of the variation within the data; 84% of variation was explained by the first four components. The plot reveals that there are three main clusters of sites, corresponding to the three zones described by their physical properties (marginal ice zone, bare ice zone and slush zone). The sites in the bare ice zone form two well-separated subclusters, one containing sites from the first ~6 km of the transect and the other containing the more distant sites (~7–50 km). This separation corresponds to the suggested organic matter wash-away and accumulation zones based on simple conceptual schemes using organic carbon concentration and quality data [25].

RDA was used to explain the variation in the chemistry and microbial data visualised in Fig. 4. Table 4 shows the results of RDA using all chemistry (Table 2) and microbial

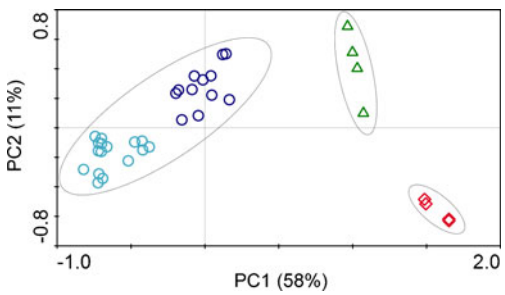

Figure 4 PCA ordination of all chemistry and microbial abundance and activity data from the transect. *Green triangles* are marginal zone sites, *red diamonds* slush zone sites and *blue circles* bare ice zone sites. *Dark blue* denotes sites from the first three bare ice zone sites, *light blue* denotes more distant sites

Table 4 Results of redundancy analysis (RDA) with manual forward selection

	% of variation explained	*p* value	*F* value
Bare ice zone	48.9	0.002	32.5
Slope	11.5	0.012	9.56
Marginal ice zone	11.2	0.012	12.6
Debris coverage	5.4	0.012	7.21
Altitude	3.7	0.038	5.74
D_{Lev}	2.3	0.046	3.82

All physical data were used as environmental variables and all chemical and microbial data used as dependent variables. Independent variables were included in the analysis according to their percentage of variation explained

D_{Lev} distance from the front of Leverett Glacier

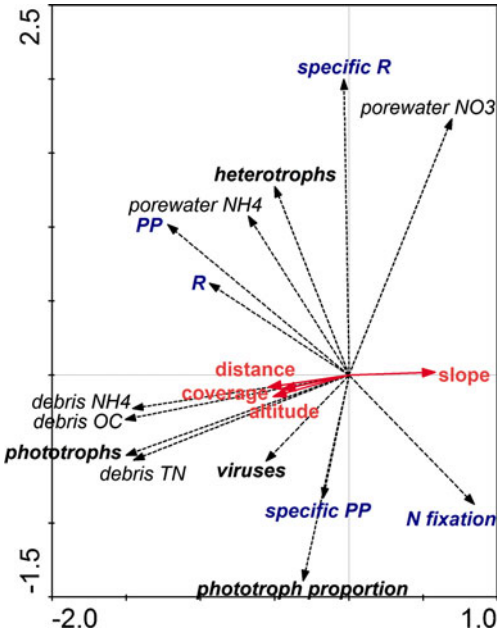

Figure 5 Redundancy analysis biplot visualising the effects of quantitative environmental variables on chemistry and microbial abundance and activity data within the bare ice zone. *Solid red arrows* denote physical variables and *dashed black arrows* dependent variables. Microbial abundance data are labelled in *bold*, activity data in *bold blue*. Some abundance data (total cells and subgroups of phototrophs) were removed from the plot for better clarity. The 'distance' *arrow* denotes the position of both D_{Lev} and D_{degl}. *PP* photosynthesis, *R* respiration

abundance and activity (Table 3) data as dependent variables and all physical data (Table 1) as independent (environmental) variables. The analysis explained a total of 86.7% of the data variation and identified six environmental variables with a significant ($p<0.05$) effect on the chemistry and microbial data (Table 4). The results corroborate the PCA ordination results and suggest that the glacier ecological zones are a major factor affecting biogeochemical processes on the ice sheet. Indeed, when only the zone variables were included in the RDA during forward selection, they explained 58% of variation (data not shown). This might distort the results of statistical analysis of the effects of quantitative environmental variables, such as distance from margin or slope. Therefore, in order to identify the most significant quantitative environmental variables, another RDA was performed using only data from the bare ice zone. Data from this zone still contained a great degree of variation, as shown in Fig. 4. Figure 5 shows a biplot of quantitative environmental variables and chemistry and microbial abundance and activity data. The analysis explained 73.3% of the total variation, with slope accounting for 35.1% ($p=0.012$), debris coverage for 13.9% ($p=0.024$) and altitude for 9.4% ($p=0.05$). There was no significant difference between the two distances used; D_{Lev} and D_{degl} explained 32.1% and 32.0% of the total variation, respectively, when included as the first variable (data not shown).

In order to test whether the variation in nutrient concentrations is a result of the physical variation or whether there exists some independent chemical variation that could affect microbial growth on the ice sheet, an RDA was performed using the chemistry data as independent and the microbial data as dependent variables, and the physical data as covariables. This analysis only explained 0.9% of the total variation in the microbial data, with no significant chemical variables identified ($p>0.05$), which suggests that the variation in the chemical environment on the ice sheet is fully explainable by the determined physical variables.

To assess the environmental controls over carbon cycling processes on the ice sheet, an RDA was performed with the carbon-related activity data (mass- and cell-related PP and R and NEP) as dependent variables and all other data used as environmental variables (Fig. 6a). This analysis explained 85% of the total variation and identified four significant controls—phototroph abundance (54.2%, $p=0.012$), proportion of phototrophs in the community (13.2%, $p=0.036$) and the abundance of Nostocales (7.3%, $p=0.046$) and Oscillatoriales (4.1%, $p=0.024$). Figure 6b shows an RDA where only physical and chemical factors (and not microbial abundance) were used as environmental variables explaining the activity data; 75.9% of the total variation was explained in this analysis, and the most significant factor was glacier ecological zone (50.1%, $p=0.026$), followed by D_{Lev} (8.8%, $p=0.03$), debris-bound OC (8.1%, $p=0.03$) and altitude (4.3%, $p=0.05$). RDA testing the significance of physical variables on net ecosystem production revealed slope as the only significant control, explaining 18.7% of the variation of all data ($p=0.012$) and 15.7% of variation in the data from the bare ice zone ($p=0.038$) (data not shown).

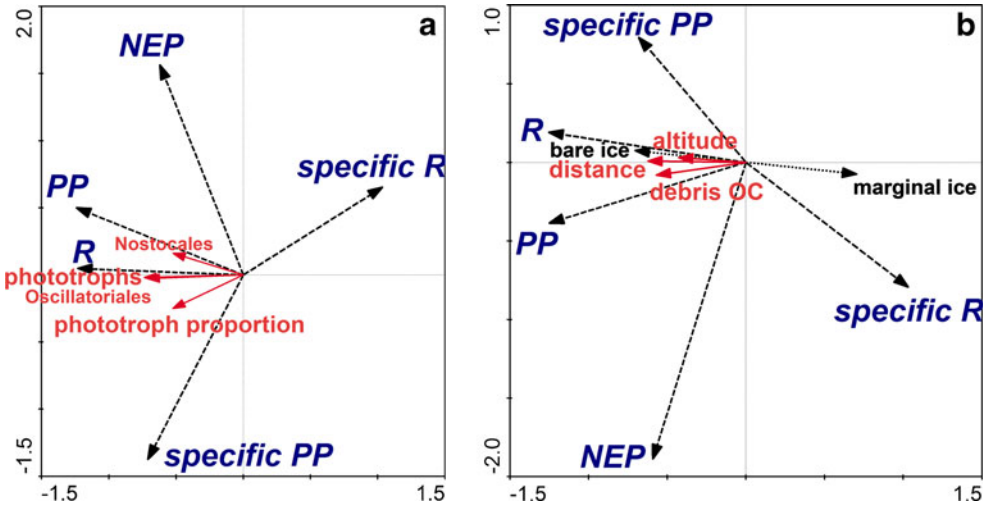

Figure 6 Redundancy analysis biplot showing the effects of **a** all physical, chemical and microbial abundance and **b** physical and chemical data on microbial carbon-related activity. *Solid red arrows* denote quantitative physical, chemical and/or microbial abundance explanatory variables, *dotted green arrows* the glacier ecological zones and *dashed black arrows* dependent variables (microbial activity, *bold blue*). Only significant explanatory variables are shown in the plots. *PP* photosynthesis, *R* respiration, *NEP* net ecosystem production

Discussion

Spatial Variability of Biogeochemical Processes on the GrIS

The first studies of the supraglacial ecosystem on the GrIS [10, 25, 33] brought evidence of significant spatial variability of organic carbon and microbial cell distribution. Moreover, the results were often counter-intuitive, with increasing carbon and nutrient concentrations up glacier, and raised questions about the spatial variability of the underlying biogeochemical processes and their controls [25]. Here we bring for the first time data on the abundance and productivity of microbes spanning the entire ablation (i.e. containing liquid water and so potentially biologically active) zone of the GrIS. We argue that the easily distinguished 'glacier ecological zones' [10] are also significantly distinct in terms of microbial activity and that proxies for wind input (D_{Lev}) and water removal (slope) provide significant controls of microbial activity within the largest bare ice zone.

The supraglacial ecosystem on the GrIS can be divided into three ecological zones, previously proposed on the basis of appearance and the presence and coverage of surface debris [10]. The ecological significance of the zones is confirmed here by the fact that they explain a major part of variation in the microbial activity on the ice sheet (Table 4, Figs. 4 and 6b). This also means that they are important to account for in ecosystem production and carbon budget estimations.

The marginal ice zone contains relatively low numbers of microbial cells and supports little activity per unit mass (Table 3). This may be due to the highly dynamic character of the glacier margin and/or the (possibly basal) source material of the surface debris [2, 10]. However, due to the high debris coverage (Table 1), the per unit area activity rates are significant (Fig. 3), and this zone should be included in future ice sheet production models.

The slush zone contains few live microbial cells due to the virtual absence of cryoconite debris (Tables 1 and 3), and its production is likely to be negligible (Figs. 2b and 3). However, runoff of snowmelt from the slush zone may be an important source of nitrogen to microorganisms in adjacent bare ice microbial communities. Furthermore, the slush zone moves from the margin up the glacier over the course of the ablation season and thus overlay each of the transect points at some point. The adsorption of snowmelt derived NH_4^+ onto cryoconite offers one explanation for the significant concentrations of cryoconite-bound nitrogen documented along the transect (Table 2) (Telling et al., submitted for publication).

The bare ice zone, the largest zone which contains developed cryoconite holes, is the most important one in terms of microbial abundance and activity, and we show that significant spatial variability in biogeochemical processes exists within this zone (Figs. 2, 3 and 4). Slope seems to be the most ecologically significant quantitative physical variable, accounting for nearly half of the variation in the data (Fig. 5). We consider slope a proxy for water flow, which is difficult to quantify directly on the glacier surface, and suggest that the action of flowing water that removes microbial cells and nutrients might be one of the principal controls of microbial activity on the ice sheet. This is supported by the negative correlation of slope and the concentration of all the measured debris-bound nutrients and the abundance of phototrophs (Fig. 5). It also corresponds with previous observations from Svalbard: Edwards et al. [5] speculated that variations in the route and rate of surface meltwater drainage may influence the availability of nutrients and microbial cells on the surface of several small glaciers, and a significant loss of OC (~70%) from cryoconite holes over the course of an

ablation season was observed on another glacier [23]. Distance from margin of the ice sheet was also a significant factor for explaining the variation in our data, and D_{Lev} (the 'wind-path distance') appeared more significant than D_{degl} in most analyses (e.g. Table 4). This supports the role of wind input as a factor affecting biogeochemical processes on large ice sheets and highlights the need for a quantitative assessment of aeolian deposition on the GrIS [25].

However, the close intercorrelation of all the physical variables is apparent in Fig. 5, and the fact that most investigated physical variables had a significant effect should be borne in mind for further interpretation. There also remains unexplained variation in the data, and it is likely that direct measurements of wind input of organic matter and/or microbial cells and of the amount of organic matter melted out of old ice [33] will provide more data relevant for supraglacial biogeochemical processes.

Controls of Net Ecosystem Production on the GrIS

Supraglacial ecosystems have been identified as potential contributors to regional and possibly global carbon cycling [1, 11], but different levels of carbon balance (i.e. autotrophy vs. heterotrophy) and origin (autochthony vs. allochthony) have been reported from them [1, 10, 23, 28]. The discrepancies were probably caused by two factors. First, different methods were employed for productivity measurements, and second, very different glaciers in terms of size and setting were worked on. The former issue has been resolved by careful testing and comparing of all available standard methods in a recent paper by Telling et al. [28], who suggested that 24-h incubations and employment of the ΔTDIC method [9] are the most appropriate for productivity measurements in Arctic supraglacial environments. We argue here that the latter suggests different environmental controls on small valley glaciers and large ice sheets, which should be taken into account in large-scale biogeochemical estimations.

The results of our productivity measurements from the transect suggest an overall net autotrophy on the GrIS (Table 3, Figs. 2b and 3). The values fit between the first estimates of Anesio et al. [1] and Hodson et al. [10] and support the proposed role of ice sheet ecosystems in carbon cycling as regional sinks of CO_2 [1] and places of production of organic matter that can be a potential source of nutrients for downstream ecosystems [11]. The results of our analysis imply that filamentous cyanobacteria (Oscillatoriales and Nostocales) are mostly responsible for primary production associated with the surface debris on the GrIS (Fig. 6a). This is supported by observations from smaller glaciers [19, 22]. Variation in the abundance of phototrophs, and thus potentially of ecosystem productivity, has also been reported from a number of glaciers and explained by altitude gradients [26, 32, 34]. Whereas this may be the case on small valley glaciers with steep altitude gradients, the effect of altitude on phototrophs on the GrIS seems to be masked by slope and distance from margin (Fig. 4).

It is likely that microbial growth and productivity in supraglacial environments is directly limited by chemical rather than physical factors. Nitrogen and phosphorus have been identified as the possible limiting nutrient in several studies from various glaciers [20, 24, 29] (Telling et al., submitted for publication). However, we show in our analysis that the variation in the chemical data is directly controlled by the physical environment, and therefore, the effect of chemistry on net ecosystem production may be skipped and the focus shifted to physical factors.

The bare ice zone is the most important area of production, with slope—the proxy for water flow—being the most significant physical control (Fig. 5). This may be at the core of the observed variation in OC distribution across the ice sheet and underlie the suggested organic matter wash-away and accumulation zones [25]. Another possible factor exerting a control over net ecosystem production and unaccounted for in our analysis is redistribution of cryoconite debris, resulting in changing light penetration and possible shifts in net productivity [4]. However, it seems that owing to lateral thermal conduction, cryoconite holes become larger and the debris layers thinner, usually resulting in a layer of single cryoconite grains, which reduces self-shading and maximises the exposure of cryoconite to solar radiation [4].

Based on the results of our analysis, we suggest that the low production estimate for the GrIS by Hodson et al. [10] may have been underestimated due to the lack of measurements higher up on the ice sheet (Figs. 2b and 3), in the 'OC accumulation zone' which is more conducive to microbial productivity, possibly due to being less perturbed by flowing water. We also show that scaling up of net ecosystem production data from small valley glaciers may yield distorted results due to shorter distance and slope gradients and, therefore, different controls of microbial activity. This may also explain the findings that most organic matter on the surface of several small Svalbard glaciers is likely to be allochthonous [23, 28]. However, given the very long times (>1,000 years) required to accumulate the present debris-bound OC far inland via microbial production only (Fig. 3), it is likely that allochthonous OC also contributes to the total OC content in the surface debris on the GrIS.

Implications for Large-Scale Production Estimations

On the basis of the results presented here, we suggest that a method applying an empirical ecosystem production model on a runoff retention model of the ice sheet should be used to

generate a credible estimate of annual production of the GrIS. The runoff retention model predicts the extension of the bare ice and slush zone (the marginal ice zone is stable) over time on the basis of meteorological data analysis [7] and was successfully used by Hodson et al. [10] for their estimate. Since there is no simple linear relationship between net ecosystem production and any one physical factor within the bare ice zone, an empirical model based on slope (the most significant physical variable) or distance (the simplest variable to use in a spatial model) could be used for refining the estimate for spatial variation within this zone.

Conclusions

We present a large dataset from a linear transect across the ablation zone of the Greenland ice sheet, consisting of physical, chemical and microbial abundance and activity data measured in summer 2010. We analyse the relationships between the physical, chemical and biological variables using multivariate statistical analysis. Concentrations of debris-bound nutrients increased with distance from margin, as did both cell numbers and activity rates before reaching a peak (photosynthesis) or a plateau (respiration, abundance) between 10 and 20 km from the ice sheet margin. The results of our productivity measurements from the transect suggest an overall net autotrophy on the GrIS and support the proposed role of ice sheet ecosystems in carbon cycling as regional sinks of CO_2 and places of production of organic matter that can be a potential source of nutrients for downstream ecosystems.

PCA based on chemical and biological data revealed three main clusters of sites, corresponding to the three glacier ecological zones, and this was confirmed by RDA using physical data as predictors. RDA using only data from the bare ice zone showed that slope accounted for most of the variation in the data. Variation in the chemical data was fully explainable by the determined physical variables. Four significant controls—phototroph abundance, proportion of phototrophs in the community and the abundance of Nostocales and Oscillatoriales—were identified for the carbon cycling-related microbial processes. Thus, we suggest that glacier ecological zones are significantly distinct in terms of microbial activity on the ice sheet and that proxies for wind input and water removal provide significant controls of microbial activity within the largest bare ice zone.

Acknowledgements This research was supported by the Marie Curie Reintegration Grant 249171 (ProGrIS) to MS and by the UK Natural Environment Research Council (NERC) grant NE/G00496X/1 to AMA. People at Camp Doom and Camp Famine are thanked for field assistance. Two anonymous reviewers are thanked for their insightful comments and criticisms.

References

1. Anesio AM, Hodson AJ, Fritz A, Psenner R, Sattler B (2009) High microbial activity on glaciers: importance to the global carbon cycle. Global Change Biol 15:955–960
2. Bøggild CE, Brandt RE, Brown KJ, Warren SG (2010) The ablation zone in northeast Greenland: ice types, albedos and impurities. J Glaciol 56:101–113
3. Bossio DA, Girvan MS, Verchot L, Bullimore J, Borelli T, Albrecht A, Scow KM, Ball AS, Pretty JN, Osborn AM (2005) Soil microbial community response to land use change in an agricultural landscape of western Kenya. Microb Ecol 49:50–62
4. Cook J, Hodson A, Telling J, Anesio A, Irvine-Fynn T, Bellas C (2010) The mass–area relationship within cryoconite holes and its implications for primary production. Ann Glaciol 51(56):106–110
5. Edwards A, Anesio AM, Rassner SM, Sattler B, Hubbard BP, Perkins WT, Young M, Griffith GW (2011) Possible interactions between bacterial diversity, microbial activity and supraglacial hydrology of cryoconite holes in Svalbard. ISME J 5:150–160
6. Foreman CM, Sattler B, Mikucki JA, Porazinska DL, Priscu JC (2007) Metabolic activity and diversity of cryoconites in the Taylor Valley, Antarctica. J Geophys Res 112:G04S32
7. Hanna E, Huybrechts P, Janssens I, Cappelen J, Steffen K, Stephens A (2005) Runoff and mass balance of the Greenland ice sheet: 1958–2003. J Geophys Res 110:D13108
8. Hodson A, Anesio AM, Ng F, Watson R, Quirk J, Irvine-Fynn T, Dye A, Clark C, McCloy P, Kohler J, Sattler B (2007) A glacier respires: quantifying the distribution and respiration CO_2 flux of cryoconite across an entire Arctic supraglacial ecosystem. J Geophys Res 112:G04S36
9. Hodson A, Cameron K, Bøggild C, Irvine-Fynn T, Langford H, Pearce D, Banwart S (2010) The structure, biological activity and biogeochemistry of cryoconite aggregates upon an Arctic valley glacier: Longyearbreen, Svalbard. J Glaciol 56:349–361
10. Hodson A, Bøggild C, Hanna E, Huybrechts P, Langford H, Cameron K, Houldsworth A (2010) The cryoconite ecosystem on the Greenland ice sheet. Ann Glaciol 51(56):123–129
11. Hood E, Fellman J, Spencer RGM, Hernes PJ, Edwards R, D'Amore D, Scott D (2009) Glaciers as a source of ancient and labile organic matter to the marine environment. Nature 462:1044–1047
12. Kaštovská K, Elster J, Stibal M, Šantrůčková H (2005) Microbial assemblages in soil microbial succession after glacial retreat in Svalbard (High Arctic). Microb Ecol 50:396–407
13. Legendre P, Legendre L (1998) Numerical ecology. Elsevier, Amsterdam, 853
14. Massieux B, Boivin MEY, van den Ende FP, Langenskiöld J, Marvan P, Barranguet C, Admiraal W, Laanbroek HJ, Zwart G (2004) Analysis of structural and physiological profiles to assess the effects of Cu on biofilm microbial communities. Appl Environ Microbiol 70:4512–4521
15. Mueller DR, Pollard WH (2004) Gradient analysis of cryoconite ecosystems from two polar glaciers. Polar Biol 27:66–74
16. Pritchard HD, Arthern RJ, Vaughan DG, Edwards LA (2009) Extensive dynamic thinning on the margins of the Greenland and Antarctic ice sheets. Nature 461:971–975
17. Ramette A (2007) Multivariate analysis in microbial ecology. FEMS Microbiol Ecol 62:142–160
18. Ramette A, Tiedje JM (2007) Multiscale responses of microbial life to spatial distance and environmental heterogeneity in a patchy ecosystem. Proc Natl Acad Sci USA 104:2761–2766
19. Säwström C, Mumford P, Marshall W, Hodson A, Laybourn-Parry J (2002) The microbial communities and primary productivity of cryoconite holes in Arctic glacier (Svalbard 79°N). Polar Biol 25:591–596

20. Säwström C, Laybourn-Parry J, Granéli W, Anesio AM (2007) Heterotrophic bacterial and viral dynamics in Arctic freshwaters: results from a field study and nutrient-temperature manipulation experiments. Polar Biol 30:1407–1415
21. Stibal M, Šabacká M, Kaštovská K (2006) Microbial communities on glacier surfaces in Svalbard: impact of physical and chemical properties on abundance and structure of cyanobacteria and algae. Microb Ecol 52:644–654
22. Stibal M, Tranter M (2007) Laboratory investigation of inorganic carbon uptake by cryoconite debris from Werenskioldbreen, Svalbard. J Geophys Res 112:G04S33
23. Stibal M, Tranter M, Benning LG, Řehák J (2008) Microbial primary production on an Arctic glacier is insignificant in comparison with allochthonous organic carbon input. Environ Microbiol 10:2172–2178
24. Stibal M, Anesio AM, Blues CJD, Tranter M (2009) Phosphatase activity and organic phosphorus turnover on a high Arctic glacier. Biogeosciences 6:913–922
25. Stibal M, Lawson EC, Lis GP, Mak KM, Wadham JL, Anesio AM (2010) Organic matter content and quality in supraglacial debris across the ablation zone of the Greenland ice sheet. Ann Glaciol 51(56):1–8
26. Takeuchi N (2001) The altitudinal distribution of snow algae on an Alaska glacier (Gulkana Glacier in the Alaska range). Hydrol Process 15:3447–3459
27. Tedesco M, Fettweis X, van den Broeke MR, van de Wal RSW, Smeets CJPP, van de Berg WJ, Serreze MC, Box JE (2011) The role of albedo and accumulation in the 2010 melting record in Greenland. Environ Res Lett 6:014005
28. Telling J, Anesio AM, Hawkings J, Tranter M, Wadham JL, Hodson AJ, Irvine-Fynn T, Yallop ML (2010) Measuring rates of gross photosynthesis and net community production in cryoconite holes: a comparison of field methods. Ann Glaciol 51(56):135–144
29. Telling J, Anesio AM, Tranter M, Irvine-Fynn T, Hodson A, Butler C, Wadham J (2011) Nitrogen fixation on Arctic glaciers, Svalbard. J Geophys Res. doi:10.1029/2010JG001632
30. ter Braak CJF (1987) Ordination. In: Jongman RHG, ter Braak CJF, van Tongeren OFR (eds) Data analysis in community and landscape ecology. Centre for Agricultural Publishing and Documentation, Wageningen, pp 91–169
31. ter Braak CJF, Šmilauer P (2002) CANOCO reference manual and CanoDraw for Windows user's guide: software for canonical community ordination (version 4.5). Microcomputer Power, Ithaca, p 550
32. Uetake J, Naganuma T, Hebsgaard MB, Kanda H, Kohshima S (2010) Communities of algae and cyanobacteria on glaciers in west Greenland. Polar Sci 4:71–80
33. Wientjes IGM, van de Wal RSW, Reichart GJ, Sluijs A, Oerlemans J (2011) Dust from the dark region in the western ablation zone of the Greenland ice sheet. Cryosphere 5:589–601
34. Yoshimura Y, Kohshima S, Ohtani S (1997) A community of snow algae on a Himalayan glacier: change of algal biomass and community structure with altitude. Arct Alp Res 29:126–137
35. Zwally HJ, Abdalati W, Herring T, Larson K, Saba J, Steffen K (2002) Surface melt-induced acceleration of Greenland ice-sheet flow. Science 297:218–222